Artificial photosynthesis and the splitting of water to generate hydrogen

*Urmimala Maitra, S. R. Lingampalli and C. N. R. Rao**

It is no exaggeration to state that the energy crisis is the most serious challenge that we face today. Among the strategies to gain access to reliable, renewable energy, the use of solar energy has clearly emerged as the most viable option. A promising direction in this context is artificial photosynthesis. In this article, we briefly describe the essential features of artificial photosynthesis in comparison with natural photosynthesis and point out the modest success that we have had in splitting water to produce oxygen and hydrogen, specially the latter.

Keywords: Hydrogen, photosynthesis, solar energy, water splitting.

THE serious energy crisis faced in the world today requires ingenious solutions and one of the important strategies would be to explore the use of solar fuels. These can be in the form of hydrogen, produced from photo-assisted water splitting, or high-energy carbon compounds such as methanol produced by the light-driven reduction of CO_2. Hydrogen has the highest energy density per unit weight, and being the cleanest source of energy is considered to be the ultimate fuel for the future, producing only water on burning. To complete the solar cycle, water must act as the only source of electrons to generate hydrogen. In this context, artificial photosynthesis has emerged as an exciting possibility and we need to find facile ways to generate oxygen and hydrogen by the oxidation/reduction of water. Photocatalytic oxygen evolution reaction involving the oxidation of water and the hydrogen evolution reaction involving the reduction of water are both important aspects related to a sunlight-based energy solution. One of the challenges that we face today with artificial photosynthesis is the development of cost-effective catalysts made of earth-abundant elements for the efficient oxidation of water to O_2 (ref. 1).

Photocatalytic water-splitting is simple in design and has been explored widely for the past several years. In photocatalytic water splitting, the energy of photons is converted to the chemical energy of H_2 by breaking the bonds in water. This process is accompanied by a large positive Gibbs free energy (238 kJ mol^{-1}). Just as in natural photosynthesis, this is an uphill reaction and is difficult to perform unlike photocatalytic degradation of organic compounds using oxygen, which is a downhill reaction. Water splitting involves two redox reactions consisting of four electrons:

Oxidation: $H_2O \rightarrow 4H^+ + O_2 + 4e^-$ (1.23 V vs SHE),

Reduction: $4H^+ + 4e^- \rightarrow H_2$ (0 V vs SHE).

Plants perform this conversion through natural photosynthesis, wherein CO_2 and water get converted to oxygen and carbohydrates. Photosynthesis occurs in two stages. In the first stage, water is oxidized to O_2 generating a proton which gets bound to $NADP^+$ to give the energy carrier, NADPH. In the second stage, NADPH is used to reduce CO_2 to glucose.

The active unit in photosystem II (PSII) in natural photosynthesis is a somewhat ill-defined Mn_4O_5Ca cluster with a $[Mn_4O_4]$ cubic unit as the core housed in a protein environment[2,3]. While the oxidation of water to produce O_2 is the more difficult step in the water-splitting reaction, the reduction of water to produce H_2 as a solar fuel is of greater interest. This can be done as in photosystem I (PSI) in plants where the reduction of protons generates energy carriers like NADPH. Semiconducting nanostructures and heterostuctures as well as dye molecules that generate electrons on photoexcitation can carry out the reduction of protons. In this article, we present a brief description of photosynthesis and highlight some of the results obtained by us on the oxidation and reduction of water, the latter enabling the generation of hydrogen.

Natural photosynthesis

In Figure 1, we show a schematic representation of natural photosynthesis. Solar energy is absorbed by chlorophyll and other pigments of PSII, which is the centre for light reaction in photosynthesis. P680 (containing

The authors are in the Chemistry and Physics Materials Unit, New Chemistry Unit and International Centre for Materials Science, Jawaharlal Nehru Centre for Advanced Scientific Research, Bangalore 560 012, India.
*For correspondence. (e-mail: cnrrao@jncasr.ac.in)

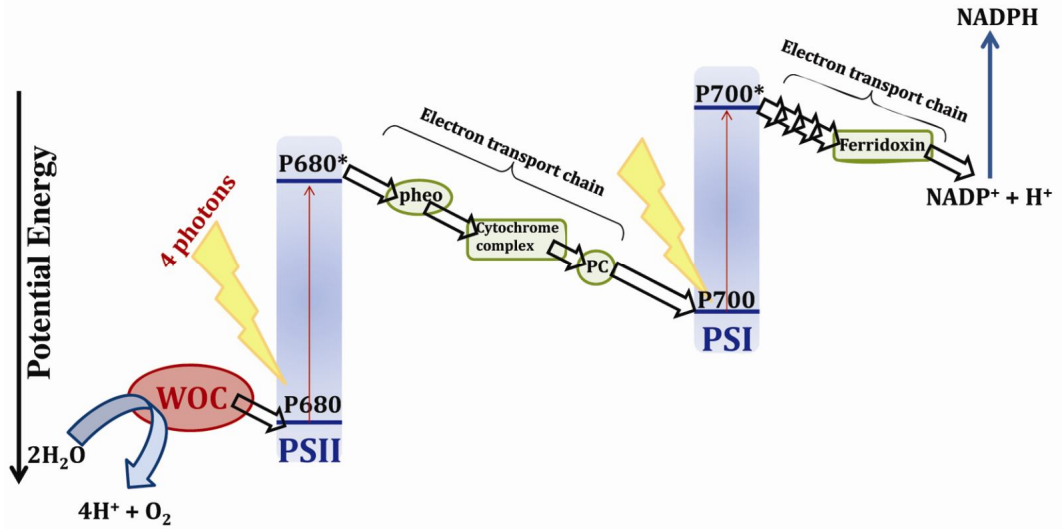

Figure 1. Z-scheme of photosynthesis. PSI and PSII are photosystems I and II respectively, also known as P680 and P700 (adapted from Tachibana *et al.*[4]).

chlorophyll *a*) or PSII absorbs a photon and loses an electron to pheophytin (a modified form of chlorophyll) generating $P680^+$. In order to reduce the probability of charge recombination, the electron is transported from pheophytin along a chain of molecules to photosystem I (PSI). This process of electron transfer down a chain of potential gradients ensures a charge separation quantum efficiency of nearly 100%, because the electron transfer processes happen on a femto-second timescale[4].

The electrons (e^-) and holes (h^+) have lifetimes of microseconds before charge recombination. $P680^+$ regains its electron from water, thereby oxidizing it to O_2 in a reaction catalysed by the water oxidizing centre (WOC) which is a cubic Mn_4O_5Ca cluster encapsulated in a protein environment. In the meantime, P700 or PSI absorbs light and loses an electron to reduce H^+ and convert $NADP^+$ to NADPH, thereby generating $P700^+$. The electron that travels down the cascade of steps to PSI is used up by $P700^+$ (ref. 4). This electron transport chain is commonly referred to as the Z-scheme of photosynthesis. Generation of O_2 from water is a four-electron process as shown in reaction 1. PSII has to therefore absorb four photons to drive this half-reaction and PSI also has to absorb four photons for the subsequent reduction reaction. Absorption of two photons by the natural photosynthetic system generates one electron and one hole, making the efficiency of this reaction almost 50%. However, considering that chlorophylls absorb nearly in the entire visible range and utilize only the red photons, the efficiency drops down to 20%. In actuality, natural photosynthesis in an agricultural crop is only 1% efficient over its entire life-cycle[5].

Artificial photosynthesis

Artificial photosynthesis provides great efficiency and simplicity and employs principles derived from natural photosynthesis. Artificial photosynthesis primarily involves a photon-absorbing centre and a catalytic centre, with an electron and hole transfer pathway joining the two. A single-step or a two-step process can be employed in artificial photosynthesis (Figure 2). In the single-step process, a photon absorber is directly attached to an electron donor on one side and/or an electron acceptor on the other. The photon absorber can be a semiconductor or a dye which absorbs light generating an electron–hole pair. The wavelength of light absorbed depends on the band gap of the semiconductor or the HOMO–LUMO gap of the dye, as shown in Figure 2 *a*. The semiconductor or dye is generally used in conjugation with an electron donor or an electron acceptor to enhance charge separation. An electron donor should have an energy level more negative than the excited state reduction potential of the semiconductor or the dye and at the same time more positive than the water oxidation potential. The electron acceptor would have an energy level more negative than the proton reduction potential and more positive than the excited state oxidation potential of the photon absorber. For swift electron transfer, acceptors and donors must be close to the photon absorber. Electron and hole transfer occurs directly from the energy levels of the semiconductor or the dye with only the electron donor or the electron acceptor, or neither of them being used in the process of the reaction.

In the two-step process, two photon absorbers are connected to each other by an electron transfer-relay material, the rest of the principles being similar to that of the single-step process, as shown in Figure 2 *b*. A redox couple issued as the electron transfer relay. The two-step process is analogous to the Z-scheme of natural photosynthesis and utilizes two photons to generate one electron and one hole. In the case of the single-step process, on the other hand, the two components of the Z-scheme

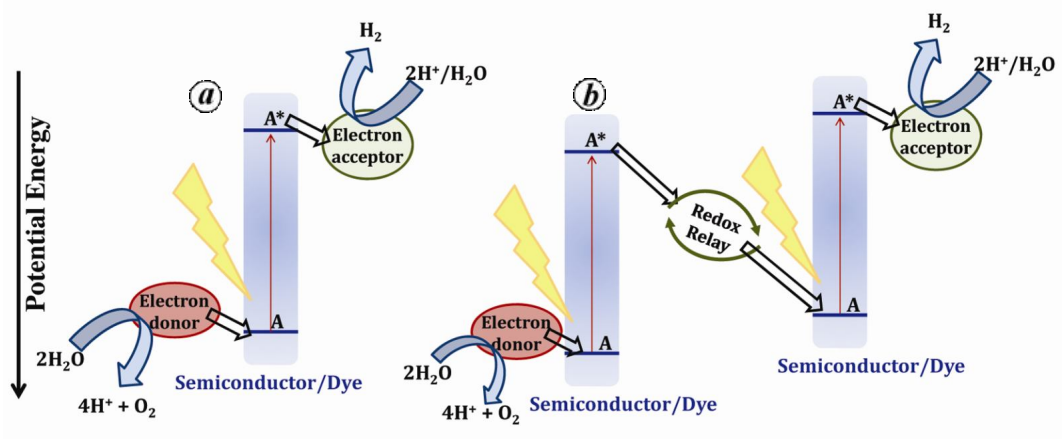

Figure 2. Artificial photosynthesis by (***a***) single- and (***b***) two-step processes (adapted from Tachibana *et al.*[4]).

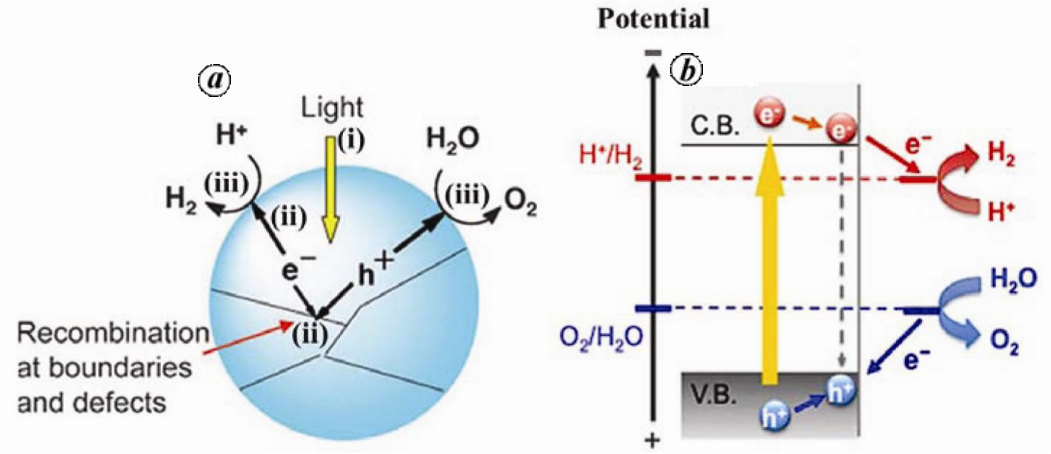

Figure 3. Schematic representations of (***a***) processes in photosynthesis and (***b***) energy-level requirements in semiconductor photocatalysis[5,8].

are combined into one. The single-step process is simple, but the disadvantage is that only a limited fraction of sunlight (< 680 nm) can be used to initiate both the oxidation and reduction of water. The two-step process can be used for complete water splitting even with low excitation energy, as low as near-infrared wavelengths. This advantage is accompanied by the difficulty of maintaining the kinetics of the full electron-transfer process with minimal energy loss by charge recombination reactions. An ideal process of electron transfer is to have more than one electron acceptor or donor level closely spaced in energy as in natural photosynthesis. However, this increases the complexity of the system and is somewhat difficult to achieve. Good electron acceptors like fullerenes[6,7] have been coupled with chromophores to achieve up to 95% charge separation. A simpler but less effective strategy is to employ co-catalysts in semiconductor-based light harvesters. Pt, NiO (for H_2) and RuO_2, IrO_2 (for O_2) satisfy the required conditions for use as catalysts.

The mechanism of photosynthesis (artificial or natural) thus comprises three aspects: (i) light-harvesting, (ii) charge generation and separation and (iii) catalytic reaction as shown in Figure 3 *a*. The photosynthetic catalysts can be classified as: semiconductor-based photocatalysts, catalysts used in photoelectrodes, dye-sensitized catalysts.

Semiconductor-based photocatalysts

These are the simplest of all catalysts, with all the three processes of photosynthesis occurring in a single system. The semiconductor absorbs a photon with energy greater than its band gap and generates an electron–hole pair, followed by the migration of the electrons and holes to the surface of the semiconductor, which participate in surface chemical reactions with water or other sacrificial agents. Recombination of e^- and h^+ competes with the process of charge separation reducing the efficiency of photocatalysis, as illustrated in Figure 3 *a*. Grain boundaries and defects in the semiconducting particles act as charge recombination centres. Charge recombination can be

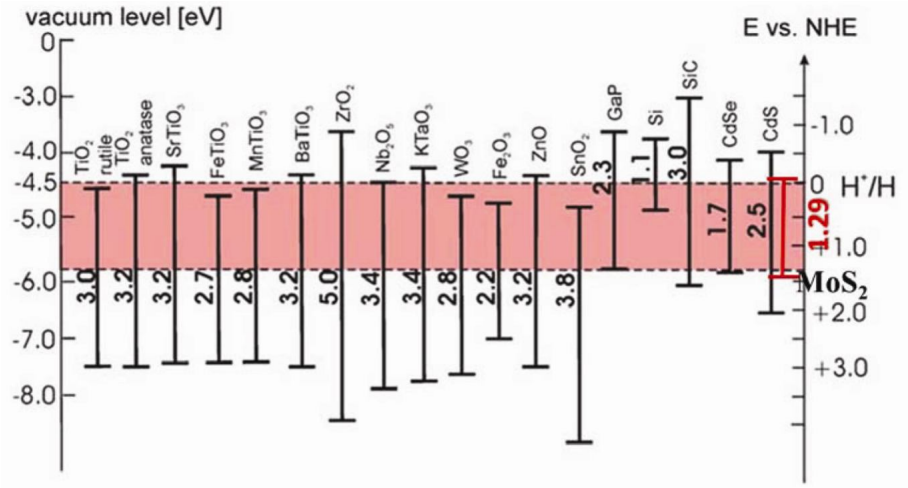

Figure 4. Some semiconductor photocatalysts and their corresponding band positions with respect to the water redox potential[9].

minimized by decreasing the size of the particle down to a few nanometres[8]. The electrons and holes would then go to the surface and are used to reduce and oxidize water respectively. They can also be used up by a sacrificial electron or hole scavenger. A hole scavenger is a strong reducing agent such as an alcohol or a sulphide, which gets reversibly oxidized by the photogenerated h^+ instead of water and thereby enriches the system with electrons to be used for the reduction of water to generate H_2. Ag^+ and Fe^{3+} have also been used as electron scavengers for water oxidation[8]. A sacrificial system eliminates back electron transfer and renders it feasible to examine only the oxidation or reduction of water.

For a semiconductor to act as a water-splitting catalyst, it must satisfy the following energy-level conditions. The bottom of the conduction band must be more negative than the reduction potential of H^+/H_2 (0 V vs SHE), and the top of the valence band must be more positive than the oxidation potential of O_2/H_2O (1.23 V), as shown in Figure 3 *b*, limiting the theoretical minimum band gap for water splitting to 1.23 eV. Based on the above criterion, several semiconductors have been identified for H_2 evolution or oxygen evolution or both (Figure 4)[9]. Semiconductors such as TiO_2, $SrTiO_3$, $BaTiO_3$, $FeTiO_3$, ZrO_2 and ZnO whose conduction band potential lies above the proton reduction potential can reduce water to produce H_2. On the other hand, semiconductors such as Fe_2O_3, SnO_2, WO_3, etc. can only oxidize water to H_2. Semiconductors like CdS, CdSe and MoS_2 are ideal for visible light photocatalytic H_2 production by virtue of the sufficiently negative conduction band potential and small band gap (Figure 4).

Catalysts used in photoelectrodes

In photo-electrocatalytic systems, the semiconductor acts as one of the electrodes of an electrochemical cell and is connected to the counter electrode via an external circuit. On absorbing light, the semiconductor generates the electron–hole pair. In the case of an n-type semiconductor photoelectrode, the photoexcited electron is transferred to the counter electrode (mostly Pt) via the external circuit, where it reduces H^+ to H_2. The h^+ oxidizes water at the semiconductor surface. In the case of a p-type semiconductor phototelectrode, the photogenerated electrons reduce water at the surface of the semiconductor while an electron from the counter electrode balances the h^+, oxidizing water at the counter electrode. The process of photo-electrochemical water splitting is demonstrated in Figure 5. Photo-electrochemical cells with both the anode and the cathode composed of photon absorbers have been used.

Even though the semiconductor possesses suitable CB/VB levels for the reduction/oxidation of water, an external bias or a pH difference (chemical bias) needs to be maintained to overcome the resistance between the two electrodes in solution and at the interface between the solution and the semiconductor electrode. Here, charge-recombination is inhibited by the bias leading to greater efficiency, with the quantum yield approaching unity and a power conversion efficiency of ~18% (ref. 10).

Dye-sensitized catalysts

Use of semiconductors as photocatalysts imposes a limitation on the band gap of the semiconductor. Semiconductors with a large band gap absorb light in the UV region, neglecting the entire visible and near-infrared regions of the solar spectrum. Dye sensitization permits the use of semiconductors with energy levels matched with the redox potential of water, without compromising on range of energies absorbed. On illumination with visible light, the excited dye transfers an electron to the conduction band of the semiconductor provided the excited state

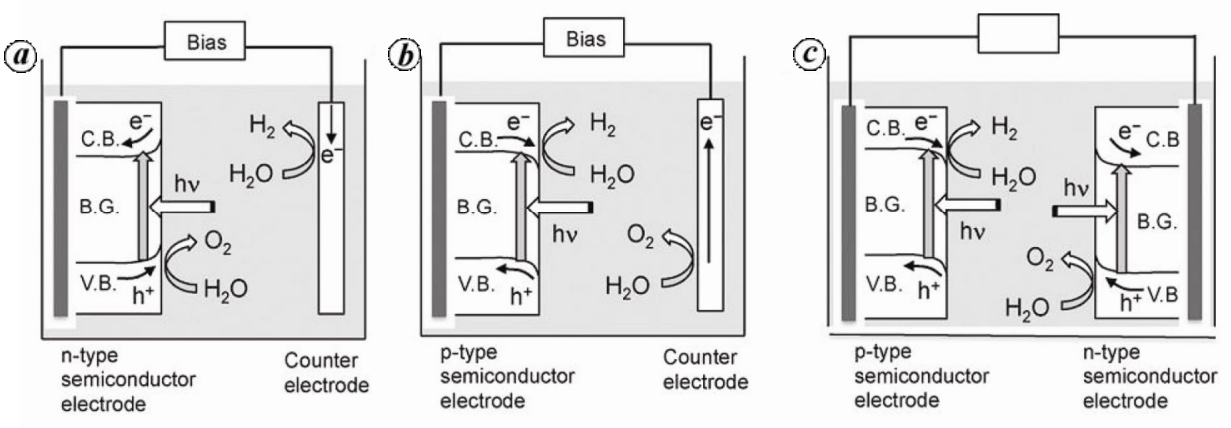

Figure 5. Schematic representation of the processes of photo-electrochemical water splitting[5].

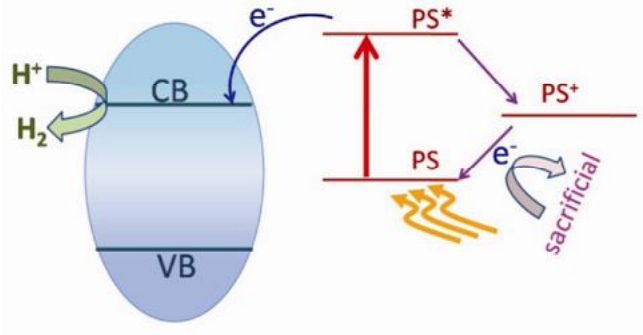

Figure 6. Schematic representation of dye-sensitized H_2 evolution (PS represents a photosensitizer/dye).

oxidation potential of the dye is more negative than the conduction band of the semiconductor (Figure 6) and the dye itself gets oxidized.

A sacrificial electron donor or a redox shuttle such as the I^{3-}/I^- pair is used to regenerate the photosensitizer and sustain the reaction cycle. Photosynthesis broadens the spectrum response range and increases the efficiency of charge transfer by spatial separation of the electron and the hole. Dye-sensitized photo-electrochemical cells having dye-sensitized photoelectrodes also work on similar principles with the reduction of water occurring at the counter electrode and the sacrificial agent getting oxidized at the photosensitized electrode. Dye-sensitized TiO_2 electrodes bearing IrO_2 nanoparticles have been used for complete water splitting. On sensitization, the dye loses an e^- to TiO_2, which transfers to the counter (Pt) electrode generating H_2. The IrO_2 particles donate e^- to the oxidized dye to regenerate the photosensitizer[11].

Water oxidation and oxygen evolution with simple inorganic catalysts

Oxidation of water, involving the transfer of four electrons has been carried out in the laboratory using efficient water oxidation catalysts such as RuO_2 and IrO_2 (although they are expensive and their availability is limited) in place of the WOC in natural photosynthesis[12–15]. The exact electronic structure of the Mn cluster in WOC is difficult to describe. However, assuming that a cubane-type Mn_4O_4 unit in WOC is important for water oxidation, Mn and Co oxides with cubane-type units such as molecular $[Mn_4O_4]$ and $[Co_4O_4]$ cubanes[16–19]. Marokite-type oxides, $CaMn_2O_4$ and $CaMn_2O_4{\cdot}xH_2O$ (refs 20 and 21) and $Ca_2Mn_3O_8$ (ref. 22), have been elucidated as water oxidation catalysts. Nanocrytalline Co_3O_4 (ref. 23) and Mn_2O_3 (ref. 24) as well as 'Co-Pi' and Co-phosphates[25,26] have also been pursued with modest successes. Two recent papers[27,28] have reported that nanoparticles of λ-MnO_2 obtained by delithiation of $LiMn_2O_4$ show a much higher water oxidation catalytic activity with a turnover frequency (TOF) of $3 \times 10^{-5}\ s^{-1}$ compared to the parent oxide. The extra flexibility of the $[Mn_4O_4]$ cubic unit in λ-MnO_2 was considered to be an important factor. Studies on nanoparticles of $Li_2Co_2O_4$ demonstrated $[Co_4O_4]$ cubic structural unit as the necessary criterion for catalytic activity[29]. Layered $LiCoO_2$, however, did not show any activity for water oxidation. Although the importance of the structure of the oxidizing unit was borne out of these studies, the actual oxidation state or the electronic configuration of the transition metal ion (Mn or Co) in water oxidation catalysis could not be delineated.

The mechanism of photocatalytic oxygen evolution by the catalysts involves $Ru(bpy)_3^{2+}$ as the sensitizer with $Na_2S_2O_8$ as the sacrificial electron acceptor in a solution buffered at pH = 5.8. Figure 7 compares natural photosynthesis with the ruthenium complex-sensitized photocatalytic water oxidation. In natural photosynthesis, chlorophyll absorbs a photon generating an excited state species which in due course reduces CO_2 to glucose. In dye-sensitized water oxidation, $Ru(bpy)_3^{2+}$ (the photon absorber) on photoexcitation donates an electron to $Na_2S_2O_8$ and itself gets oxidized to $Ru(bpy)_3^{3+}$. $Ru(bpy)_3^{3+}$ takes up an electron from the catalyst, just as

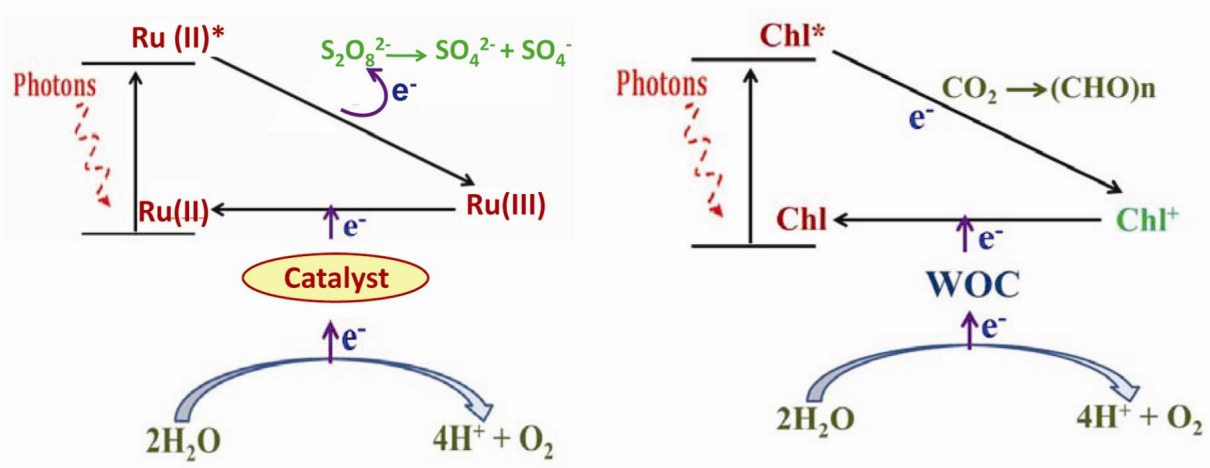

Figure 7. Comparison of mechanism of photocatalytic water oxidation (left) with natural photosynthesis (right).

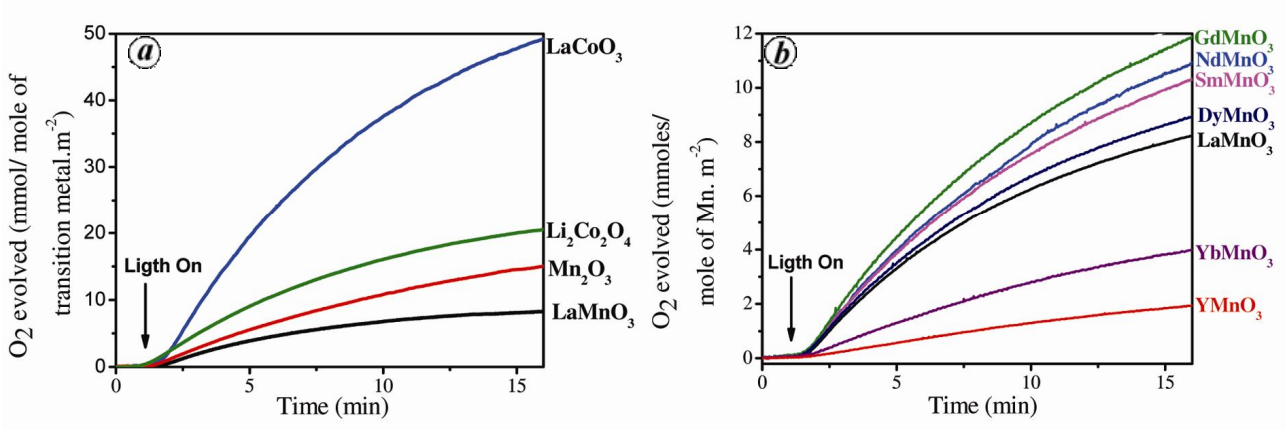

Figure 8. Oxygen evolution activity of (***a***) different Mn and Co oxide catalysts and (***b***) cubic and hexagonal rare manganites[30,31].

oxidized chlorophyll does from the WOC. The catalyst or WOC regains its electrons by oxidizing water.

A recent study of the photocatalytic oxygen evolution reaction by Mn and Co oxides has shown that those oxides with trivalent Mn and Co ions possessing e_g^1 electronic configuration were most active for oxygen evolution reaction (Figure 8 *a*)[30]. Thus, Mn_2O_3, $LaMnO_3$ and $MgMn_2O_4$, all of which contain Mn in +3 state with $t_{2g}^3e_g^1$ configuration show good catalytic activity even though all of them exist in different crystal structures. Hexagonal perovskite manganites containing Mn^{+3} do not show good catalytic activity, the Mn in these oxides having the electronic configuration of $e''^2 2e'^2 a_a'^0$ (Figure 8 *b*)[31]. Similarly, $LaCoO_3$, $Li_2Co_2O_4$ and solid solutions of Co^{3+} in Ln_2O_3 all show high catalytic activity (Figure 8 *a*), Co in these catalysts being in the +3 oxidation state with the $t_{2g}^5e_g^1$ configuration[30].

Table 1 shows the oxygen evolution activity of some of the transition metal oxides. It is clear that irrespective of structure of the transition metal, the electronic configuration of the transition metal plays a crucial role in determining oxygen evolution activity, e_g^1 electron being a crucial criterion. The ability of the e_g orbital to form σ-bonds with anion adsorbates aids the binding of oxygen-related intermediate species. A single electron in the e_g orbital is likely to yield just the appropriate strength of interaction between O_2 and the catalyst for oxygen evolution reaction[32,33].

Proton reduction and hydrogen evolution

Proton reduction is carried out naturally by the hydrogenase enzyme that catalyses the reduction of protons accompanied by the oxidation of electron donors such as ferridoxin. Recently, it has become possible to anchor hydrogenase to an electrode surface[34], synthesize compounds in solution resembling the hydrogenase active site and showing activity for hydrogen evolution[35,36].

Of all the hydrogen evolution catalysts, semiconductor-based photocatalysts with the semiconductor acting as both the photon absorber and catalyst are the simplest in

Table 1. Comparison of O_2 evolution activities (turnover frequencies; TOF) of different transition metal oxide catalysts[30,31]

Catalyst	Crystal structure	Electronic configuration	TOF/s^{-1}	Catalyst	Crystal structure	Electronic configuration	TOF/s^{-1}
$LaFeO_3$	Perovskite	$t_{2g}^3e_g^2$	8.9×10^{-5}	λ-MnO_2	Spinel	$t_{2g}^3e_g^0$	2.2×10^{-5}
$LaMnO_3$	Perovskite	$t_{2g}^3e_g^1$	4.8×10^{-4}	Mn_2O_3	Bixbyte	$t_{2g}^3e_g^1$	5×10^{-4}
$LaCoO_3$	Perovskite	$t_{2g}^5e_g^1$	1.4×10^{-3}	$MgMn_2O_4$	Spinel	$t_{2g}^3e_g^1$	0.8×10^{-4}
$LaNiO_3$	Perovskite	$t_{2g}^6e_g^1$	1.2×10^{-4}	$Li_2Co_2O_4$	Spinel	$t_{2g}^5e_g^1$	9×10^{-4}
$DyCoO_3$	Perovskite	$t_{2g}^5e_g^1$	2.8×10^{-4}	$(Er_2O_3)(Co_2O_3)$	Solid solution	$t_{2g}^5e_g^1$	1.3×10^{-3}

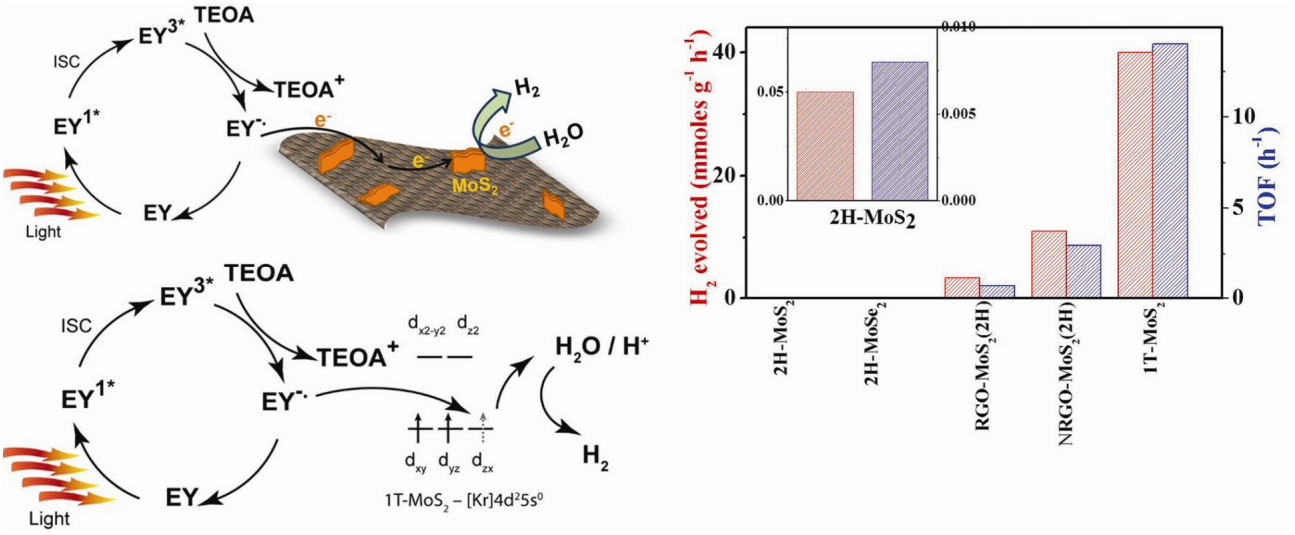

Figure 9. Schematics of dye-sensitized H_2 evolution over graphene-MoS_2 composites and 1T-MoS_2 along with a bar diagram showing comparative H_2 evolution activity of different MoS_2 based catalysts (adapted from Maitra *et al.*[57]).

design. In 1980, Scaife[37] noted that it is intrinsically difficult to develop an oxide semiconductor photocatalyst that satisfies both the conditions of having sufficiently negative conduction band for H_2 production and a sufficiently narrow band gap for visible light absorption. This is because of the highly positive valance bands (+3.0 V vs NHE) in oxides formed of the O 2p orbitals. Non-oxide semiconductors like sulphides and nitrides possess appropriate band levels for visible light-induced H_2 evolution. Nitrogen doping in large band gap oxides like TiO_2 makes them photocatalytically active in the visible region[38–41]. Co-doping of F with N in TiO_2 helps retain the charge balance and reduce defects, thereby reducing the probability of electron–hole recombination and increasing the photocatalytic H_2 evolution yield[42]. Oxynitrides specially those of Ta and Nb, show high visible light photocatalysis based on similar principles[43–46].

MoS_2 has a free energy for H_2 evolution comparable to that of nitrogenase and hydrogenase with the edge structure of MoS_2 sheets having close resemblance with the catalytically active sites of these enzymes. MoS_2 has proven to be a good catalyst for electrochemical as well as photochemical hydrogen evolution reaction (HER)[47–49]. Theoretical and experimental studies indicate that edges of MoS_2 are catalytically active, while the basal plane remains inert[50,51]. Nanoparticles of MoS_2 with single-layered truncated triangular morphology and exposed Mo edges[51,52], or those grown on highly ordered pyrolytic graphite[53] or graphitic carbon[54,55] show electrochemical H_2 evolution. Hydrogen evolution appears to be further enhanced using graphene[56] or carbon nanotubes[47] to support nanocrystalline MoS_2, the favourable conductivity of the nanocarbons ensuring efficient electron transfer to the electrodes. Recently, photocatalytic dye-sensitized H_2 evolution has been reported for MoS_2 and its composite with graphene[57–59]. Figure 9 shows the H_2 evolution activity of MoS_2 and its composites[57]. While MoS_2 by itself shows very low H_2 evolution, its composite with graphene (RGO–MoS_2) shows good catalysis, with graphene acting as a conductive substrate for the efficient transfer of the photogenerated electrons to MoS_2, thereby increasing the lifetime of the photogenerated electrons. Nitrogen doping of graphene (NRGO) enhances the electron-donating ability of graphene and almost doubles the catalytic yield[57].

The reaction of dye-sensitized water splitting with MoS_2 involves photosensitization of the dye EY to generate reactive species EY^-, which then can donate one electron to the catalyst[59]. The final reaction is

$$H_2O + e^- \rightarrow \tfrac{1}{2}H_2 + OH^-.$$

Although the overall reaction is photocatalytic generation of H_2, the electrons that are involved in the reduction of

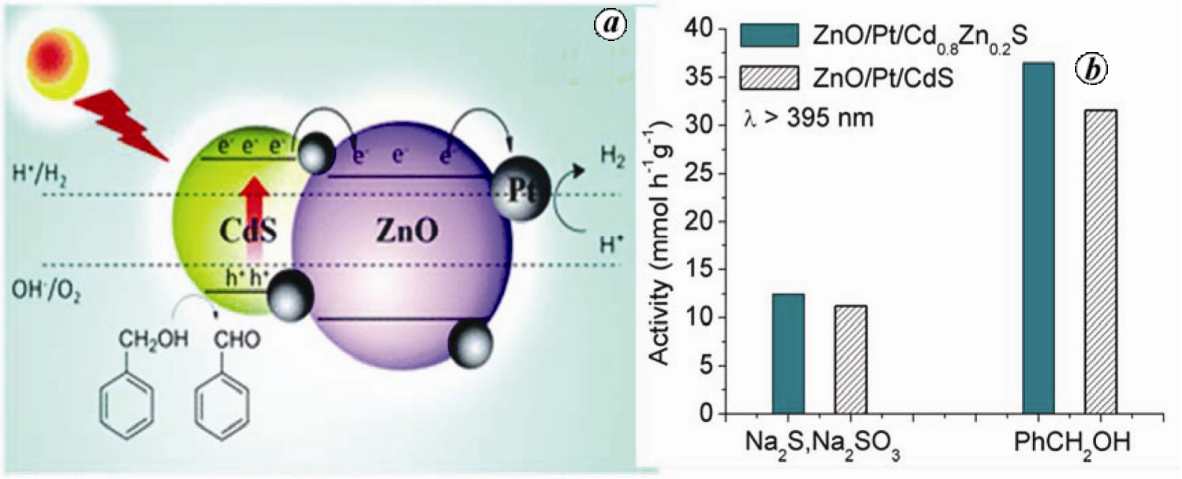

Figure 10. ***a***, Schematic representation of the formation of ZnO/Pt/CdS nanohetero-structures in H_2 generation. ***b***, Photocatalytic hydrogen evolution activities of ZnO/Pt/CdS with ZnO/Pt/$Cd_{0.8}Zn_{0.2}S$ in the presence of Na_2S and Na_2SO_3 and benzyl alcohol in acidic medium under visible light irradiation (adapted from Lingampalli *et al.*[63]).

H_2O are not photocatalytically generated on MoS_2, rather transferred from the photogenerated species EY^- to MoS_2. Based on the above principle, it is found that if MoS_2 itself is rendered metallic thereby increasing its conductivity, it shows high catalytic activity. 1T-MoS_2, the structural polytype of semiconducting 2H-MoS_2 is metallic and shows activity about 600–1000 times that of 2H-MoS_2 (Figure 9). Likewise, 1T-$MoSe_2$ shows extraordinarily high catalytic activity, being the best catalyst by far[57].

Use of semiconductor heterostructures

One of the important features in semiconductor artificial photosynthesis is the manner in which one can have the electrons and the holes apart, accomplished by semiconductor heterostructures. Amirav and Alivisatos[60] have employed the CdSe seeded CdS nanorods with Pt tip for photocatalytic hydrogen production. In this system, photogenerated electrons were received by Pt and catalysed the water reduction, and the holes were transferred to the CdS to carry out methanol oxidation. Several other hetero-structures such as ZnO/CdS/Pt (ref. 61) and TiO_2/CdS/Pt (ref. 62) have been designed for photocatalytic hydrogen evolution.

Hybrid nanoheterostructures of the type ZnO/Pt/CdS have been prepared recently by a simple solution process[63]. The process involved deposition of Pt nanoparticles on ZnO, followed by the deposition of CdS nanoparticles. A schematic representation of charge transfer and catalytic reaction is shown in Figure 10 *a*, a noteworthy feature being the presence of Pt nanoparticles between ZnO and CdS nanoparticles. In these nanostructures, photogenerated charges in the CdS are separated by transferring electrons to ZnO. Pt deposited on ZnO acts as an electron sink, thereby promoting proton reduction. Holes retained on the CdS were utilized in the oxidation of sacrificial agents. The photocatalytic hydrogen evolution was further improved by substitution of Zn in CdS as in ZnO/Pt/$Cd_{0.8}Zn_{0.2}S$ and Se in CdS as in ZnO/Pt/$CdS_{0.5}Se_{0.5}$ under visible as well as UV–visible light irradiation in the presence of Na_2S and Na_2SO_3. The activity further improves using benzyl alcohol in acidic medium as the sacrificial agent (Figure 10 *b*). The improved efficiency in these systems is achieved due to the efficient charge separation by the nanoheterostructures. Semiconductor heterostructures with ZnO and TiO_2, partly substituted with N and F, would be even more effective in H_2 reduction.

Conclusion

The discussion in the earlier sections should suffice to justify the expectation that artificial photosynthesis and splitting of water can provide a viable solution to the energy problem by enabling the production of hydrogen using solar energy. There have been sizable demonstrations of the fairly large-scale production of hydrogen using semiconductor nanostructures and other means. It would be especially useful if the decomposition of water can be carried out thermally at reasonable temperatures (600–800°C) using solar energy. Clearly, research in the area of water-splitting is worthy of greater effort.

1. Pace, R. J., In *Artificial Photosynthesis*, Wiley-VCH Verlag GmbH & Co, KGaA, Weinheim, Germany, 2005, pp. 13–34.
2. Yachandra, V., DeRose, V., Latimer, M., Mukerji, I., Sauer, K. and Klein, M., Where plants make oxygen: a structural model for the photosynthetic oxygen-evolving manganese cluster. *Science*, 1993, **260**, 675–679.

3. Penner-Hahn, J., In *Metal Sites in Proteins and Models Redox Centres, Vol. 90: Structure and Bonding* (eds Hill, H. A. O., Sadler, P. J. and Thomson, A. J.), Springer, Berlin, 1998, ch. 1, pp. 1–36.
4. Tachibana, Y., Vayssieres, L. and Durrant, J. R., Artificial photosynthesis for solar water-splitting. *Nature Photonics*, 2012, **6**, 511–518.
5. Abe, R., Recent progress on photocatalytic and photoelectrochemical water splitting under visible light irradiation. *J. Photochem. Photobiol. C*, 2010, **11**, 179–209.
6. González-Rodríguez, D., Carbonell, E., Rojas, G. D. M., Castellanos, C. A., Guldi, D. M. and Torres, T., Activating multistep charge-transfer processes in fullerene–subphthalocyanine–ferrocene molecular hybrids as a function of π–π orbital overlap. *J. Am. Chem. Soc.*, 2010, **132**, 16488–16500.
7. Kodis, G., Liddell, P. A., Moore, A. L., Moore, T. A. and Gust, D., Synthesis and photochemistry of a carotene–porphyrin–fullerene model photosynthetic reaction center. *J. Phys. Org. Chem.*, 2004, **17**, 724–734.
8. Kudo, A. and Miseki, Y., Heterogeneous photocatalyst materials for water splitting. *Chem. Soc. Rev.*, 2009, **38**, 253–278.
9. Batzill, M., Fundamental aspects of surface engineering of transition metal oxide photocatalysts. *Energy Environ. Sci.*, 2011, **4**, 3275–3286.
10. Kleinfeld, E. R. and Ferguson, G. S., Stepwise formation of multilayered nanostructural films from macromolecular precursors. *Science*, 1994, **265**, 370–373.
11. Youngblood, W. J., Lee, S.-H. A., Maeda, K. and Mallouk, T. E., Visible light water splitting using dye-sensitized oxide semiconductors. *Acc. Chem. Res.*, 2009, **42**, 1966–1973.
12. Lee, Y., Ye, B.-U., Yu, H. K., Lee, J.-L., Kim, M. H. and Baik, J. M., Facile synthesis of single crystalline metallic RuO_2 nanowires and electromigration-induced transport properties. *J. Phys. Chem. C*, 2011, **115**, 4611–4615.
13. Marshall, A. T. and Haverkamp, R. G., Electrocatalytic activity of IrO_2–RuO_2 supported on Sb-doped SnO_2 nanoparticles. *Electrochim. Acta*, 2010, **55**, 1978–1984.
14. Lee, Y., Suntivich, J., May, K. J., Perry, E. E. and Shao-Horn, Y., Synthesis and activities of rutile IrO_2 and RuO_2 nanoparticles for oxygen evolution in acid and alkaline solutions. *J. Phys. C. Lett.*, 2012, **3**, 399–404.
15. Di Blasi, A. *et al.*, Preparation and evaluation of RuO_2–IrO_2, IrO_2–Pt and IrO_2–Ta_2O_5 catalysts for the oxygen evolution reaction in an SPE electrolyzer. *J. Appl. Chem.*, 2009, **39**, 191–196.
16. McCool, N. S., Robinson, D. M., Sheats, J. E. and Dismukes, G. C., A Co_4O_4 'Cubane' water oxidation catalyst inspired by photosynthesis. *J. Am. Chem. Soc.*, 2011, **133**, 11446–11449.
17. Symes, M. D., Lutterman, D. A., Teets, T. S., Anderson, B. L., Breen, J. J. and Nocera, D. G., Photo-active cobalt cubane model of an oxygen-evolving catalyst. *ChemSusChem.*, 2013, **6**, 65–69.
18. Dismukes, G. C., Brimblecombe, R., Felton, G. A. N., Pryadun, R. S., Sheats, J. E., Spiccia, L. and Swiegers, G. F., Development of bioinspired Mn_4O_4–cubane water oxidation catalysts: lessons from photosynthesis. *Acc. Chem. Res.*, 2009, **42**, 1935–1943.
19. Brimblecombe, R., Koo, A., Dismukes, G. C., Swiegers, G. F. and Spiccia, L., Solar driven water oxidation by a bioinspired manganese molecular catalyst. *J. Am. Chem. Soc.*, 2010, **132**, 2892–2894.
20. Najafpour, M. M., Ehrenberg, T., Wiechen, M. and Kurz, P., Calcium manganese(III) oxides ($CaMn_2O_4{\cdot}xH_2O$) as biomimetic oxygen-evolving catalysts. *Angew. Chem., Int. Ed. Engl.*, 2010, **49**, 2233–2237.
21. Zaharieva, I., Najafpour, M. M., Wiechen, M., Haumann, M., Kurz, P. and Dau, H., Synthetic manganese–calcium oxides mimic the water-oxidizing complex of photosynthesis functionally and structurally. *Energy Environ. Sci.*, 2011, **4**, 2400–2408.
22. Ramírez, A., Bogdanoff, P., Friedrich, D. and Fiechter, S., Synthesis of $Ca_2Mn_3O_8$ films and their electrochemical studies for the oxygen evolution reaction (OER) of water. *Nano Energy*, 2012, **1**, 282–289.
23. Jiao, F. and Frei, H. Nanostructured cobalt oxide clusters in mesoporous silica as efficient oxygen-evolving catalysts. *Angew. Chem., Int. Ed. Engl.*, 2009, **48**, 1841–1844.
24. Jiao, F. and Frei, H., Nanostructured manganese oxide clusters supported on mesoporous silica as efficient oxygen-evolving catalysts. *Chem. Commun.*, 2010, **46**, 2920–2922.
25. Kanan, M. W., Yano, J., Surendranath, Y., Dincă, M., Yachandra, V. K. and Nocera, D. G., Structure and valency of a cobalt–phosphate water oxidation catalyst determined by *in situ* X-ray spectroscopy. *J. Am. Chem. Soc.*, 2010, **132**, 13692–13701.
26. Zhong, D. K. and Gamelin, D. R., Photoelectrochemical water oxidation by cobalt catalyst ('Co–Pi')/α-Fe_2O_3 composite photoanodes: oxygen evolution and resolution of a kinetic bottleneck. *J. Am. Chem. Soc.*, 2010, **132**, 4202–4207.
27. Robinson, D. M., Go, Y. B., Greenblatt, M. and Dismukes, G. C., Water oxidation by λ-MnO_2: catalysis by the cubical Mn_4O_4 subcluster obtained by delithiation of spinel $LiMn_2O_4$. *J. Am. Chem. Soc.*, 2010, **132**, 11467–11469.
28. Robinson, D. M. *et al.*, Photochemical water oxidation by crystalline polymorphs of manganese oxides: structural requirements for catalysis. *J. Am. Chem. Soc.*, 2013, **135**, 3494–3501.
29. Gardner, G. P. *et al.*, Structural requirements in lithium cobalt oxides for the catalytic oxidation of water. *Angew. Chem., Int. Ed. Engl.*, 2012, **51**, 1616–1619.
30. Maitra, U., Naidu, B. S., Govindaraj, A. and Rao, C. N. R., Importance of trivalency and the e_g^1 configuration in the photocatalytic oxidation of water by Mn and Co oxides. *Proc. Natl. Acad. Sci. USA*, 2013, **110**(29), 11704–11707.
31. Naidu, B. S., Gupta, U., Maitra, U. and Rao, C. N. R., Visible light induced oxidation of water by rare earth manganites, cobaltites and related oxides. *Chem. Phys. Lett.*, 2014, **591**, 277–281.
32. Suntivich, J., May, K. J., Gasteiger, H. A., Goodenough, J. B. and Shao-Horn, Y., A perovskite oxide optimized for oxygen evolution catalysis from molecular orbital principles. *Science*, 2011, **334**, 1383–1385.
33. Suntivich, J., Gasteiger, H. A., Yabuuchi, N., Nakanishi, H., Goodenough, J. B. and Shao-Horn, Y., Design principles for oxygen-reduction activity on perovskite oxide catalysts for fuel cells and metal-air batteries. *Nature Chem.*, 2011, **3**, 647–647.
34. Lamle, S. E., Vincent, K. A., Halliwell, L. M., Albracht, S. P. J. and Armstrong, F. A., Hydrogenase on an electrode: a remarkable heterogeneous catalyst. *Dalton Trans.*, 2003, 4152–4157; DOI: 10.1039/B306234C.
35. Rauchfuss, T. B., Research on soluble metal sulfides: from polysulfido complexes to functional models for the hydrogenases. *Inorg. Chem.*, 2003, **43**, 14–26.
36. Mejia-Rodriguez, R., Chong, D., Reibenspies, J. H., Soriaga, M. P. and Darensbourg, M. Y., The hydrophilic phosphatriazaadamantane ligand in the development of H_2 production electrocatalysts: iron hydrogenase model complexes. *J. Am. Chem. Soc.*, 2004, **126**, 12004–12014.
37. Scaife, D. E., Oxide semiconductors in photoelectrochemical conversion of solar energy. *Solar Energy*, 1980, **25**, 41–54.
38. Zhang, Z. *et al.*, Band-gap tuning of N-doped TiO_2 photocatalysts for visible-light-driven selective oxidation of alcohols to aldehydes in water. *RSC Adv.*, 2013, **3**, 7215–7218.
39. Balcerski, W., Ryu, S. Y. and Hoffmann, M. R., Visible-light photoactivity of nitrogen-doped TiO_2: photo-oxidation of HCO_2H to CO_2 and H_2O. *J. Phys. Chem. C*, 2007, **111**, 15357–15362.
40. Irie, H., Watanabe, Y. and Hashimoto, K., Nitrogen-concentration dependence on photocatalytic activity of $TiO_{2-x}N_x$ powders. *J. Phys. Chem. B*, 2003, **107**, 5483–5486.

41. Sathish, M., Viswanathan, B., Viswanath, R. P. and Gopinath, C. S., Synthesis, characterization, electronic structure, and photocatalytic activity of nitrogen-doped TiO_2 nanocatalyst. *Chem. Mater.*, 2005, **17**, 6349–6353.
42. Kumar, N., Maitra, U., Hegde, V. I., Waghmare, U. V., Sundaresan, A. and Rao, C. N. R., Synthesis, characterization, photocatalysis, and varied properties of TiO_2 cosubstituted with nitrogen and fluorine. *Inorg. Chem.*, 2013, **52**, 10512–10519.
43. Abe, R., Higashi, M. and Domen, K., Facile fabrication of an efficient oxynitride TaON photoanode for overall water splitting into H_2 and O_2 under visible light irradiation. *J. Am. Chem. Soc.*, 2010, **132**, 11828–11829.
44. Higashi, M., Domen, K. and Abe, R., Highly stable water splitting on oxynitride TaON photoanode system under visible light irradiation. *J. Am. Chem. Soc.*, 2012, **134**, 6968–6971.
45. Siritanaratkul, B., Maeda, K., Hisatomi, T. and Domen, K., Synthesis and photocatalytic activity of perovskite niobium oxynitrides with wide visible-light absorption bands. *ChemSusChem.*, 2011, **4**, 74–78.
46. Maeda, K. and Domen, K., New non-oxide photocatalysts designed for overall water splitting under visible light. *J. Phys. Chem. C*, 2007, **111**, 7851–7861.
47. Laursen, A. B., Kegnaes, S., Dahl, S. and Chorkendorff, I., Molybdenum sulfides-efficient and viable materials for electro- and photoelectrocatalytic hydrogen evolution. *Energy Environ. Sci.*, 2012, **5**, 5577–5591.
48. Tributsch, H. and Bennett, J. C., Electrochemistry and photochemistry of MoS_2 layer crystals. I. *J. Electroanal. Chem. Interfacial. Electrochem.*, 1977, **81**, 97–111.
49. Sakamaki, K., Hinokuma, K. and Fujishima, A., Photoelectrochemical *in situ* observation of n-MoS_2 in aqueous solutions using a scanning tunneling microscope. *J. Vacuum Sci. Technol. B*, 1991, **9**, 944–949.
50. Hinnemann, B. *et al.*, Biomimetic hydrogen evolution: MoS_2 nanoparticles as catalyst for hydrogen evolution. *J. Am. Chem. Soc.*, 2005, **127**, 5308–5309.
51. Jaramillo, T. F., Jørgensen, K. P., Bonde, J., Nielsen, J. H., Horch, S. and Chorkendorff, I., Identification of active edge sites for electrochemical H_2 evolution from MoS_2 nanocatalysts. *Science*, 2007, **317**, 100–102.
52. Helveg, S. *et al.*, Atomic-scale structure of single-layer MoS_2 nanoclusters. *Phys. Rev. Lett.*, 2000, **84**, 951–954.
53. Kibsgaard, J., Lauritsen, J. V., Lægsgaard, E., Clausen, B. S., Topsøe, H. and Besenbacher, F., Cluster-support interactions and morphology of MoS_2 nanoclusters in a graphite-supported hydrotreating model catalyst. *J. Am. Chem. Soc.*, 2006, **128**, 13950–13958.
54. Brorson, M., Carlsson, A. and Topsøe, H., The morphology of MoS_2, WS_2, Co–Mo–S, Ni–Mo–S and Ni–W–S nanoclusters in hydrodesulfurization catalysts revealed by HAADF-STEM. *Catal. Today*, 2007, **123**, 31–36.
55. Bonde, J., Moses, P. G., Jaramillo, T. F., Norskov, J. K. and Chorkendorff, I., Hydrogen evolution on nano-particulate transition metal sulfides. *Faraday Discuss.*, 2009, **140**, 219–231.
56. Li, Y., Wang, H., Xie, L., Liang, Y., Hong, G. and Dai, H., MoS_2 nanoparticles grown on graphene: an advanced catalyst for the hydrogen evolution reaction. *J. Am. Chem. Soc.*, 2011, **133**, 7296–7299.
57. Maitra, U., Gupta, U., De, M., Datta, R. and Rao, C. N. R., Highly effective visible-light induced H_2 generation by single-layer 1T-MoS_2 and a nanocomposite of few-layer 2H-MoS_2 with heavily nitrogenated graphene. *Angew. Chem., Int. Ed. Engl.*, 2013, **52**, 13057–13061; 10.1002/anie.201306918
58. Zong, X. *et al.*, Visible light driven H_2 production in molecular systems employing colloidal MoS_2 nanoparticles as catalyst. *Chem. Commun.*, 2009, 4536–4538.
59. Min, S. and Lu, G., Sites for high efficient photocatalytic hydrogen evolution on a limited-layered MoS_2 cocatalyst confined on graphene sheets – the role of graphene. *J. Phys. Chem. C*, 2012, **116**, 25415–25424.
60. Amirav, L. and Alivisatos, A. P., Photocatalytic hydrogen production with tunable nanorod heterostructures. *J. Phys. Chem. Lett.*, 2010, **1**, 1051–1054.
61. Wang, X., Liu, G., Chen, Z.-G., Li, F., Wang, L., Lu, G. Q. and Cheng, H.-M., Enhanced photocatalytic hydrogen evolution by prolonging the lifetime of carriers in ZnO/CdS heterostructures. *Chem. Commun.*, 2009, 3452–3454.
62. Park, H., Choi, W. and Hoffmann, M. R., Effects of the preparation method of the ternary CdS/TiO_2/Pt hybrid photocatalysts on visible light-induced hydrogen production. *J. Mater. Chem.*, 2008, **18**, 2379–2385.
63. Lingampalli, S. R., Gautam, U. K. and Rao, C. N. R., Highly efficient photocatalytic hydrogen generation by solution-processed ZnO/Pt/CdS, ZnO/Pt/$Cd_{1-x}Zn_xS$ and ZnO/Pt/$CdS_{1-x}Se_x$ hybrid nanostructures. *Energy Environ. Sci.*, 2013; DOI: 10.1039/c1033ee42623h.

Received 14 November 2013; accepted 24 January 2014